Report
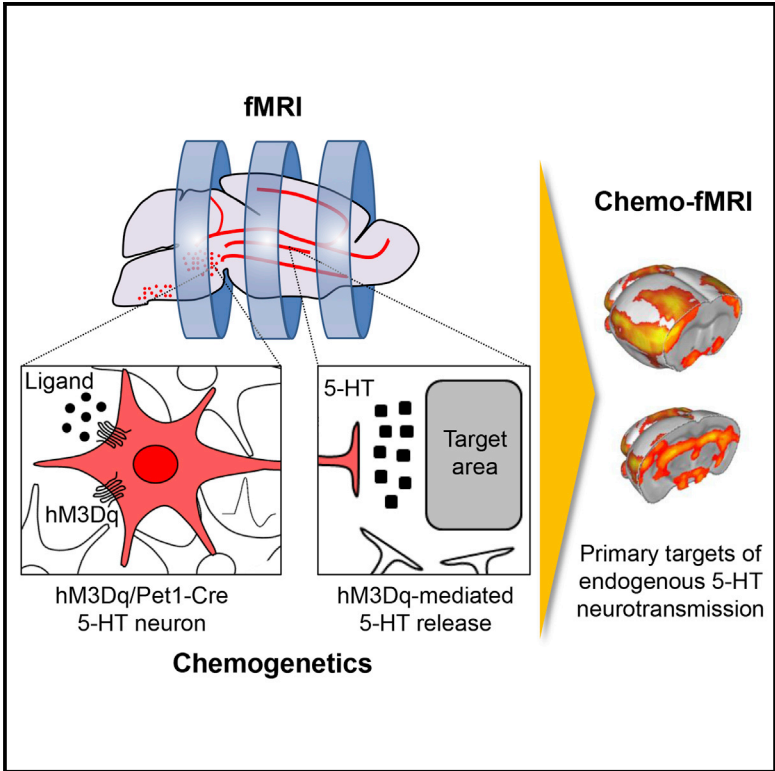
Brain-wide Mapping of Endogenous Serotonergic Transmission via Chemogenetic fMRI

Graphical Abstract

Authors

Andrea Giorgi, Sara Migliarini,
Alberto Galbusera, ..., Raffaella Tonini,
Alessandro Gozzi, Massimo Pasqualetti

Correspondence

alessandro.gozzi@iit.it

In Brief

Giorgi et al. combined chemogenetics and functional magnetic resonance imaging (chemo-fMRI) to establish causation between serotonin release and regional functional activity. They show that endogenous serotonergic transmission does not affect global brain activity but selectively activates a set of target regions that serve as primary effectors of this modulatory system.

Highlights

- We describe a combination of chemogenetics and mouse fMRI (chemo-fMRI)

- Chemogenetic release of serotonin activates a set of primary regional effectors

- Systemic serotonin boosting results in widespread deactivation

- Chemo-fMRI can be used to causally manipulate evoked and intrinsic brain activity

CrossMark

CellPress

Brain-wide Mapping of Endogenous Serotonergic Transmission via Chemogenetic fMRI

Andrea Giorgi,[1,2] Sara Migliarini,[2] Alberto Galbusera,[1] Giacomo Maddaloni,[2] Maddalena Mereu,[3] Giulia Margiani,[3] Marta Gritti,[4] Silvia Landi,[5,6] Francesco Trovato,[5,6] Sine Mandrup Bertozzi,[7] Andrea Armirotti,[7] Gian Michele Ratto,[5,6] Maria Antonietta De Luca,[3] Raffaella Tonini,[4] Alessandro Gozzi,[1,8,9,*] and Massimo Pasqualetti[1,2,8]

[1]Functional Neuroimaging Laboratory, Center for Neuroscience and Cognitive Systems, Istituto Italiano di Tecnologia, 38068 Rovereto, Italy
[2]Biology Department, University of Pisa, 56127 Pisa, Italy
[3]Biomedical Sciences Department, University of Cagliari, 09124 Cagliari, Italy
[4]Neuroscience and Brain Technologies Department, Istituto Italiano di Tecnologia, 16163 Genova, Italy
[5]Institute Nanoscience, National Research Council, 56127 Pisa, Italy
[6]Scuola Normale Superiore, 56127 Pisa, Italy
[7]D3 Pharmachemistry, Istituto Italiano di Tecnologia, 16163 Genova, Italy
[8]Senior author
[9]Lead Contact
*Correspondence: alessandro.gozzi@iit.it
 https://doi.org/10.1016/j.celrep.2017.09.087

SUMMARY

Serotonin-producing neurons profusely innervate brain regions via long-range projections. However, it remains unclear whether and how endogenous serotonergic transmission specifically influences regional or global functional activity. We combined designed receptors exclusively activated by designed drugs (DREADD)-based chemogenetics and functional magnetic resonance imaging (fMRI), an approach we term "chemo-fMRI," to causally probe the brain-wide substrates modulated by endogenous serotonergic activity. We describe the generation of a conditional knockin mouse line that, crossed with serotonin-specific Cre-recombinase mice, allowed us to remotely stimulate serotonergic neurons during fMRI scans. We show that endogenous stimulation of serotonin-producing neurons does not affect global brain activity but results in region-specific activation of a set of primary target regions encompassing corticohippocampal and ventrostriatal areas. By contrast, pharmacological boosting of serotonin levels produced widespread fMRI deactivation, plausibly reflecting the mixed contribution of central and perivascular constrictive effects. Our results identify the primary functional targets of endogenous serotonergic stimulation and establish causation between activation of serotonergic neurons and regional fMRI signals.

INTRODUCTION

Serotonin (5-HT) is a modulatory transmitter produced by a small set of midbrain and brainstem nuclei that richly innervate forebrain target regions via long-range projections (Maddaloni et al., 2017). Such profuse innervation, along with the combined release of transmitters via pointwise synaptic signaling as well as non-synaptic "volume transmission" (Descarries and Mechawar, 2000), can alter neuronal functions to define internal states that affect behavioral outputs in response to external stimuli. Recent research has shed light on the basic cellular and molecular machinery engaged by serotonin (Lesch and Waider, 2012). However, many questions regarding the systems-level substrates modulated by serotonin transmission remain unanswered. For one, it is unclear whether serotonin's modulatory action entails a global regulation of neural activity or is relayed and encoded by a set of primary functional targets.

Neuroimaging studies have employed pharmacological manipulations to probe the brain-wide targets of serotonin. The vast majority of these studies have primarily focused on the use of functional magnetic resonance imaging (fMRI) as a proxy for the neuronal activity directly elicited by pharmacological agents or by mapping second-order modulatory effects on task-elicited fMRI responses (Anderson et al., 2008). This approach, termed pharmacological fMRI, has also been back-translated to animal studies (Klomp et al., 2012). However, while useful in identifying possible brain-wide substrates of neuromodulatory action, drug-based approaches are often contaminated by off-target receptor contributions (Ofek et al., 2012) and often contain peripheral vasotonic or cerebrovascular contributions that cannot be easily disentangled from the drug's primary neural effects (Martin and Sibson, 2008). This aspect is especially relevant when hemodynamic measures of brain function are used, given that serotonin can perivascularly modulate blood flow, independent of its central effects (Cohen et al., 1996). As a result, it remains unclear where and how endogenous serotonergic activity specifically influences regional or global brain functional activity and the corresponding fMRI responses.

Light-based or chemically mediated cell manipulations have made it possible to causally link the activity of focal neuronal populations with specific circuital and behavioral outputs (Park and Carmel, 2016). When combined with non-invasive
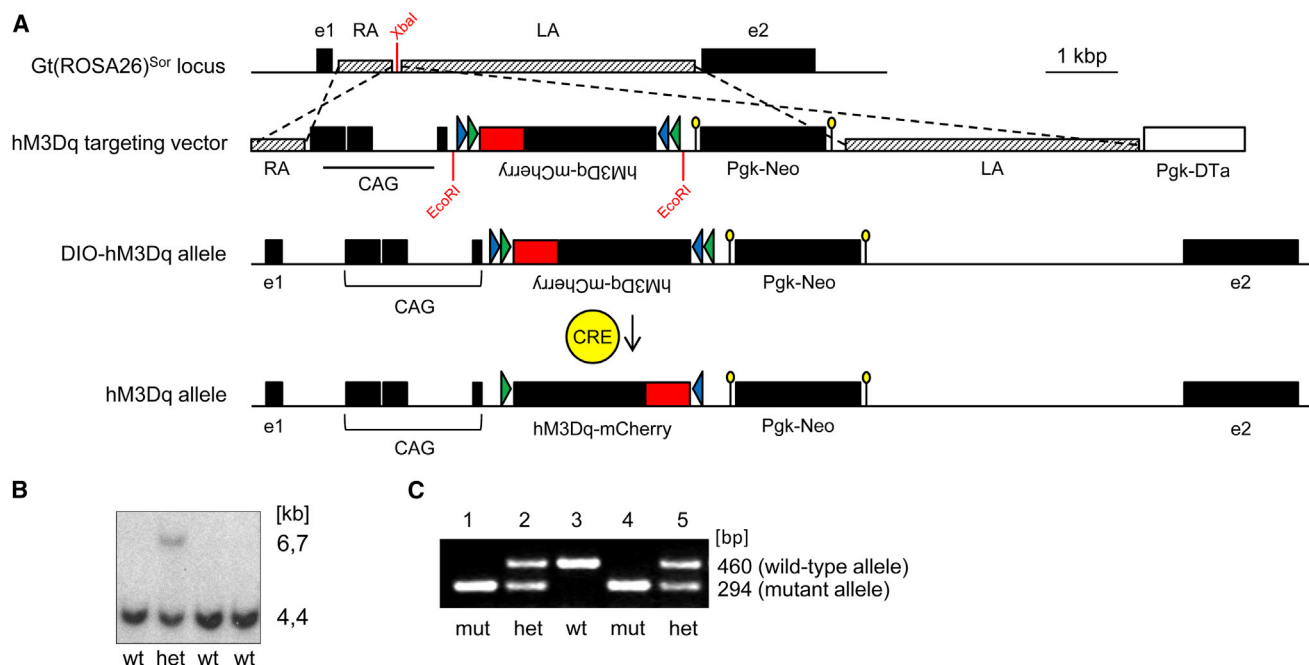
Figure 1. Generation of the hM3Dq Conditional Knockin Mouse Line

Targeted integration of the hM3Dq construct in the ROSA26 genomic locus.

(A) Top to bottom: wild-type organization of ROSA26 mouse genomic locus; hM3Dq targeting vector (green, *loxP*; blue, Lox2722; arrowheads indicate the location of Lox sites, and yellow circles indicate FRT sites); transcriptionally inactive DIO-hM3Dq allele; and transcriptionally active hM3Dq allele.

(B) Southern blot analysis of genomic DNA extracted from embryonic stem cells clones after HindIII digestion (hM3Dq allele = 6.7 kb; wild-type allele = 4.4 kb).

(C) PCR amplification of the ROSA26 locus from DNA extracted from a wild-type mouse (3), two mutant mice (1 and 4), and two heterozygous DIO-hM3Dq mice (2 and 5).

neuroimaging methods, cell-type-specific manipulations can be used to map the functional substrates of endogenous modulatory transmission without the confounding contribution of peripherally elicited vasoactive or pharmacological effects. Toward this goal, we describe the combined use of mouse cerebral-blood-volume-based fMRI (rCBV; Galbusera et al., 2017) and cell-type-specific DREADD (designed receptors exclusively activated by designed drugs; Armbruster et al., 2007) chemogenetics, an approach we term "chemo-fMRI," to map the brain-wide functional targets of sustained serotonin stimulation.

To allow for stable and reproducible endogenous serotonin stimulation across animals, we generated a conditional knockin mouse that we crossed with Pet1-Cre transgenic mice (Pelosi et al., 2014), endowing serotonin specificity (Spencer and Deneris, 2017). This approach allowed us to remotely stimulate serotonin-producing neurons during fMRI scans, with reduced inter-subject variability. Our results show that chemogenetic serotonin stimulations do not affect global brain activity but result in region-specific activation of a set of primary target regions encompassing corticohippocampal and midbrain structures, as well as components of the mesolimbic reward systems. Notably, pharmacological boosting of serotonin level via systemic administration of the serotonin reuptake inhibitor citalopram produced widespread fMRI deactivation, plausibly reflecting the mixed contribution of central and perivascular constrictive effects. Collectively, our results reveal a set of

regional substrates that act as primary functional targets of endogenous serotonergic stimulation and establish causation between endogenous activation of serotonin neurons and regional fMRI signals. They also provide a framework for understanding serotonin-dependent functions and interpreting data obtained from human fMRI studies of serotonin modulating agents.

RESULTS

hM3Dq-Mediated Modulation of Serotonergic Neurons

To enable stable pan-neuronal stimulation of serotonin-producing cells, we first generated an hM3Dq conditional knockin mouse encompassing the integration of hM3Dq-mCherry double-floxed inverse open reading frame (DIO-hM3Dq) within the ROSA26 genomic locus (Figure 1). In the designed mouse line, stable Cre-mediated somatic recombination is required for conditional transcriptional activation (CAG-promoter driven) of the hM3Dq gene, whose expression could be probed by the presence of in-frame-fused mCherry reporter (Figure 1). To enable hM3Dq expression in serotonin-producing neurons, DIO-hM3Dq mice were crossed with the $Pet1_{210}$-Cre transgenic mouse line (Pelosi et al., 2014). Immunofluorescence analysis on double trans-heterozygous hM3Dq/Pet1-Cre mice revealed that hM3Dq is expressed in the vast majority (95.9%) of serotonin-producing neurons (Figures 2A–2D′).

We next recorded the electrophysiological response induced by clozapine-N-oxide (CNO) administration in hM3Dq-expressing serotonin neurons via whole-cell patch-clamp recordings in the dorsal raphe nucleus (DRN). mCherry-positive neurons in hM3Dq/Pet1-Cre mice were robustly activated by CNO, resulting in sustained firing rates (Figure 2E). We did not observe any CNO-induced firing rate alterations in any of the neighboring mCherry-negative neurons probed or in serotonin neurons in DIO-hM3Dq control mice (Figures 2F and 2G).

Chemo-fMRI Mapping of Endogenous Serotonin Neurotransmission

To control for possible off-target effects of CNO and its metabolites, we first performed a dose-response titration of the fMRI response produced by CNO in wild-type mice (Figure S1). Intravenous CNO administration at doses of 1 and 2 mg/kg produced significant rCBV increases in most of the examined regions (Figure S1; $p < 0.05$, corrected at $q = 0.05$). Upon intravenous dosing of CNO at 0.5 mg/kg, the rCBV signal was qualitatively distinguishable from reference baseline signal only in hypothalamic and hippocampal areas, and no statistically significant alterations were detected in regional or voxelwise quantifications with respect to vehicle ($p > 0.42$, $Z > 1.6$ in voxelwise maps). Pharmacokinetic profiling of this dose (Figure S1C) revealed sustained plasma CNO exposure throughout the imaging time window, as well as the presence of low but detectable levels of clozapine. The observed peak exposure of clozapine (8 ± 6 ng/mL) is ~25-fold lower than behaviorally relevant plasma levels of this compound in rodents (Olsen et al., 2008) and below the range of values previously associated with detectable brain exposure (Baldessarini et al., 1993). Based on these assessments, we chose to perform subsequent chemogenetic-fMRI mapping using an i.v. dose of 0.5 mg/kg. As a further control for possible CNO/clozapine off-target effects, fMRI mapping and all the supporting experiments were performed and quantified by administering CNO to both hM3Dq/Pet1-Cre and control DIO-hM3Dq reference mice. CNO administration did not alter peripheral blood pressure at any of the doses tested (Figure S2).

Chemogenetic activation of serotonin-producing neurons elicited robust rCBV increases in several cortical and non-cortical substrates in hM3Dq/Pet1-Cre mice (Figure 3; $Z > 2$, cluster corrected $p = 0.05$; Figure S3). The elicited chemo-fMRI response encompassed parietal cortical and motor cortices, as well as posterior insular and temporal association regions, plus several subcortical substrates, including hippocampal areas, the hypothalamus, the dorsal raphe, and the cerebellum. A prominent involvement of ventral tegmental area and its mesolimbic terminals in the nucleus accumbens was also apparent.

To probe a neural origin of hM3Dq-mediated fMRI response, we performed local field potential (LFP) measurements in the dorsal hippocampus of halothane-anesthetized animals (Galbusera et al., 2017). Intravenous (i.v.) CNO administration (0.5 mg/kg) produced significant LFP power increases in the theta ($F_{1,22} = 110.2$, $p < 0.001$) and gamma bands ($F_{1,22} = 239.4$, $p < 0.001$) in hM3Dq/Pet1-Cre, but not in DIO-hM3Dq control animals (Figure S4). To rule out an interaction between the anesthesia used for fMRI and serotonin chemogenetic manipulations, we carried out c-Fos immunofluorescence mapping

in unanesthetized mice upon intraperitoneal administration of 2 mg/kg CNO (see dose selection in Supplemental Experimental Procedures). This dosing strategy does not elicit substantial fMRI signal alterations (Figure S5; $p > 0.26$, all regions). We observed robust and recognizable increases in c-Fos-positive neurons in many regional substrates identified with fMRI, including the nucleus accumbens, hippocampus, anterior thalamus, hypothalamic nuclei, and raphe nuclei (Figure S6A–S6E; $p < 0.05$, all regions, $q = 0.05$). No inter-group differences were observed in somatosensory cortex (Figures S6A–S6E), and no detectable c-Fos reactivity was observed in the cerebellum in either CNO-treated group (data not shown). The same dose of CNO (2 mg/kg i.p.) elicited significant release of extracellular serotonin in hM3Dq/Pet1-Cre animals, but not in DIO-hM3Dq control animals, as assessed with hippocampal microdialysis in unanesthetized animals (Figure S6F; $F_{1,10} = 7.76$, $p = 0.02$).

Systemic Serotonin Reuptake Inhibition Produces fMRI Deactivation

An underlying assumption of our work is that the signals elicited by CNO in hM3Dq/Pet1-Cre mice primarily reflect central serotonin neuronal stimulation, which in turn elicits rCBV changes via neurovascular and neurometabolic coupling. By contrast, fMRI mapping of systemically administered serotonin ligands may be contaminated or masked by direct stimulation of endothelial serotonin receptors, which produces vasoconstrictive responses (Cohen et al., 1996). To compare the effect of endogenous versus systemic pharmacological serotonin stimulation, we carried out fMRI mapping upon administration of the selective serotonin reuptake inhibitor citalopram (5–10 mg/kg), a drug leading to increased central and circulating serotonin levels (Blardi et al., 2005). Interestingly, i.v. citalopram (10 mg/kg) produced widespread foci of rCBV signal decrease in a widespread set of cortical and subcortical regions, as seen with voxelwise mapping (Figure S7; $Z > 1.8$, cluster corrected $p = 0.05$). Although the effect was widely distributed, the deactivation was particularly prominent in the prefrontal cortex (Figures 4B and S7). Citalopram administration was not associated with appreciable blood pressure alteration at any of the doses tested (Figure S2).

DISCUSSION

Serotonin is an archetypical neuromodulatory monoamine characterized by broad and far-ranging modulatory properties. Despite extensive research, the macroscale functional substrates endogenously modulated by serotonin in the intact brain remain elusive. By using chemo-fMRI, we describe the primary brain-wide targets of sustained serotonergic stimulation and establish causation between endogenous activation of serotonin neurons and regional fMRI signals. Our results provide a framework for understanding serotonin-dependent function and interpreting data obtained from human fMRI studies of serotonin modulatory agents.

While the density of serotonin ascending projections is highly variable across neuroanatomical regions, virtually no area in the CNS is devoid of serotonin innervation (Maddaloni et al., 2017). Our observation of region-specific responses in spite of the
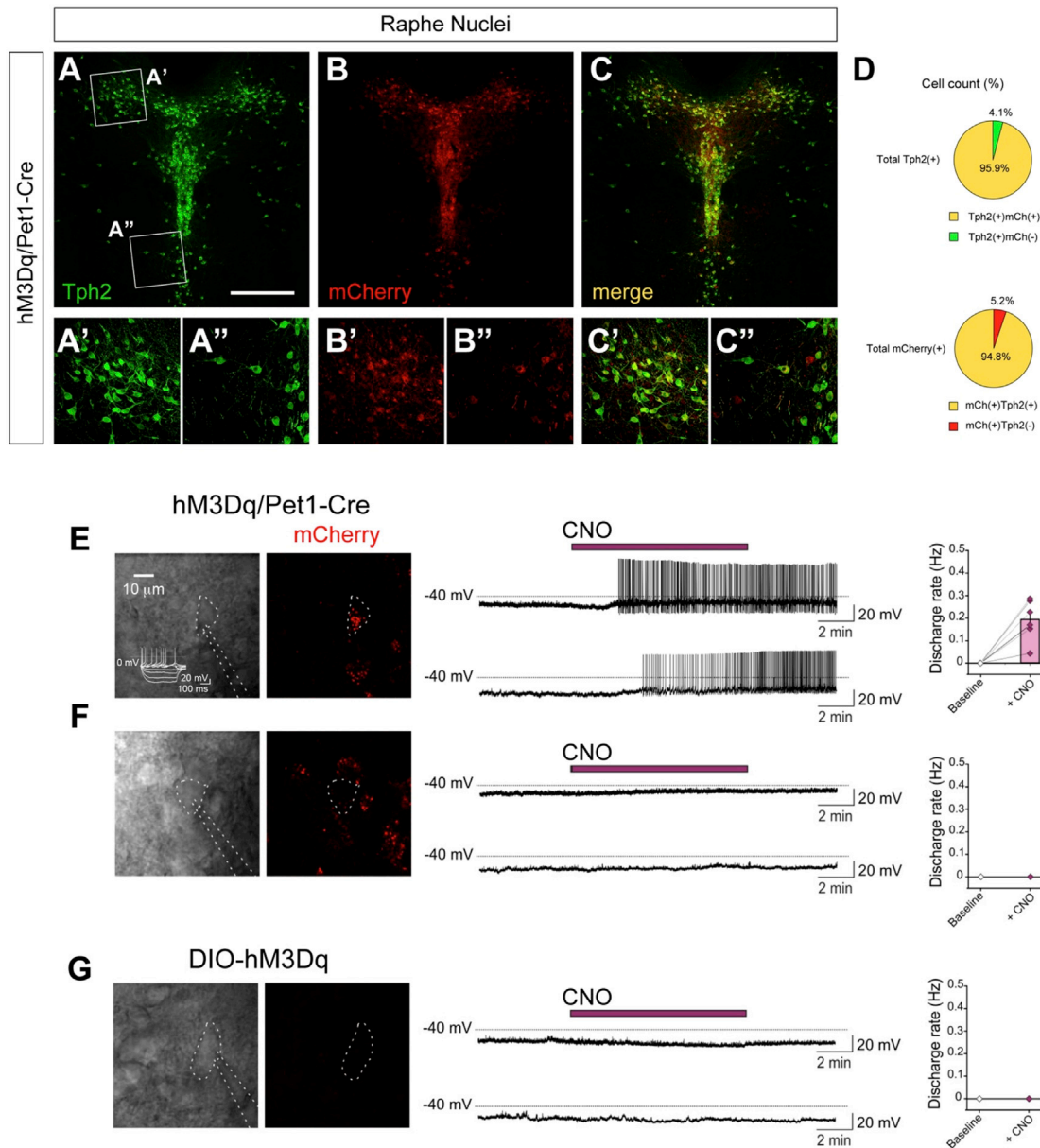
Figure 2. hM3Dq Expression in Serotonin Neurons and Electrophysiological Validation

(A–C) Double immunohistochemical assay showing Tph2 (A) and mCherry expression (B) and merged channels (C) in medial and dorsal raphe nucleus (MRN and DRN, respectively) of hM3Dq/Pet1-Cre mice (n = 4).

(A′–C″) High-power magnification highlighting Tph2 (A′) and mCherry (B′) co-localization (C′) in the DRN lateral wings, and Tph2 (A″) and mCherry (B″) co-localization (C″) in MRN.

(D) Quantification of hM3Dq-expressing serotonin neurons.

(E) CNO application (5 µM, purple bar) in DRN brain slices from hM3Dq/Pet1-Cre mice triggered firing activity in mCherry(+)serotonin neurons (discharge rate, 0.19 ± 0.03 Hz; p = 0.003), identified by their electrophysiological properties (inset). CNO did not elicit activity in mCherry(−) cells (F) or DIO-hM3Dq control cells (G). (E–G) Left, image of recorded cells; middle, sample traces of recorded cell membrane potential; right, boxplot summary of changes in discharge rate in response to CNO application.

Scale bars represent 380 µm (A–C) and 150 µm (A′–C″).

use of drug-like pan-serotonergic stimulation provides evidence that endogenous serotonin neurotransmission engages a set of neuroanatomical targets that serve as primary, fast-responding effectors of sustained release of this neurotransmitter. This notion is consistent with a role of serotonin as a mediator of arousal (Lee and Dan, 2012) and species-normative consummatory behaviors that strongly engage evolutionary-ancient ventrolimbic substrates (Takahashi et al., 2012; Liu et al., 2014). The
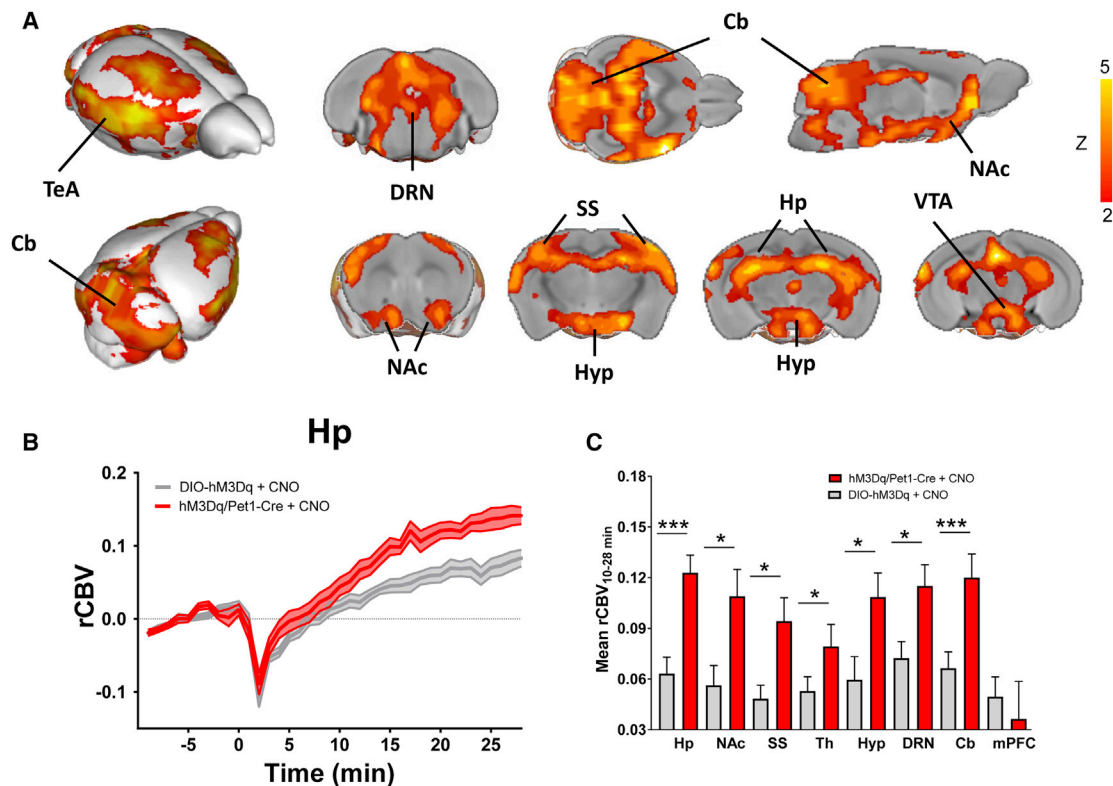
Figure 3. fMRI Response to Chemogenetic Stimulation of Serotonergic Neurons
fMRI activation produced by intravenous (i.v.) CNO administration (0.5 mg/kg) in hM3Dq/Pet1-Cre mice (n = 20) and CNO-treated DIO-hM3Dq controls (n = 14).
(A) Anatomical distribution of the brain regions activated in hM3Dq/Pet1-Cre mice (Z > 2, cluster corrected at p = 0.05).
(B) Illustrative fMRI time course in the hippocampus; CNO was administered at time 0 (mean ± SEM).
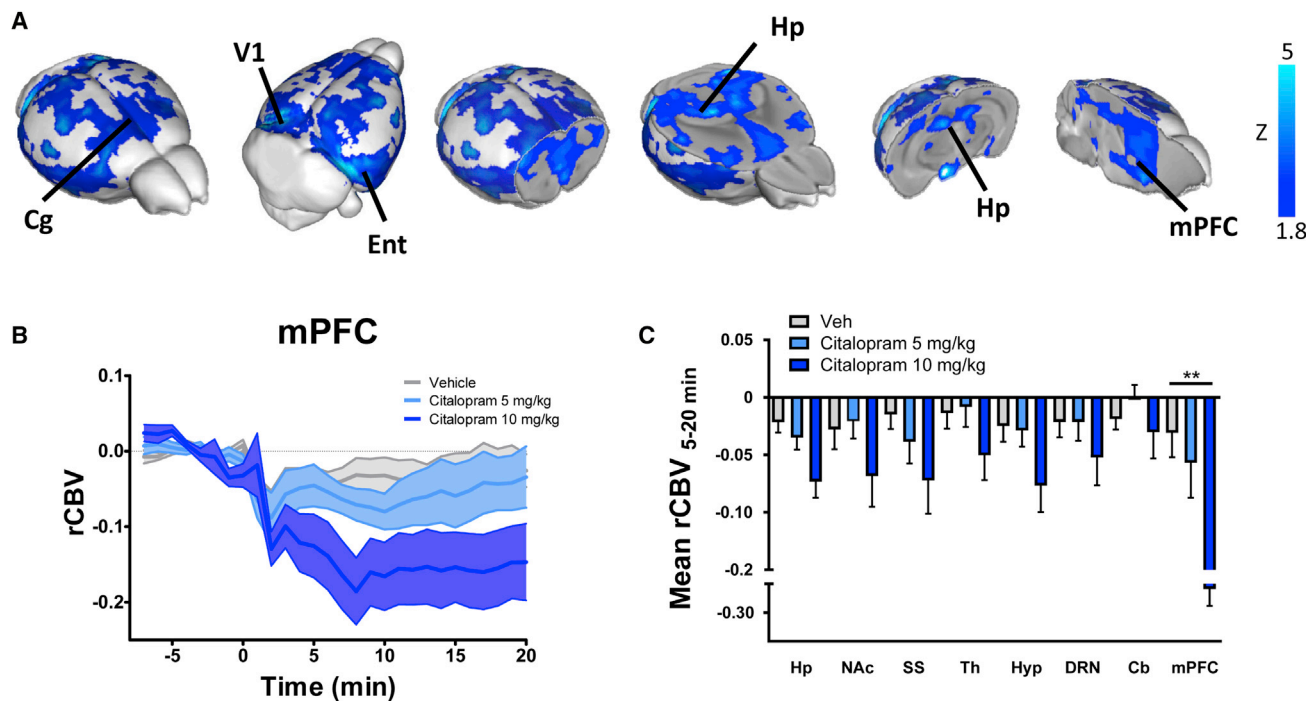(C) rCBV quantification in representative volumes of interest (mean ± SEM; *p < 0.05, **p < 0.01, corrected at q = 0.05).
Cb, cerebellum; DRN, dorsal raphe nucleus; Hp, hippocampus; Hyp, hypothalamus; mPFC, prefrontal cortex; NAc, nucleus accumbens; SS, somatosensory cortex; Th, thalamus.

presence of parietocortical activation is in keeping with the result of metabolic and cerebral blood flow mapping upon electrical or chemical stimulation of raphe regions (Cohen et al., 1996; Underwood et al., 1995). While the robust activation of hippocampal, hypothalamic, and midbrain areas is consistent with the especially dense serotonin innervation of these areas, qualitative comparisons with prior fiber or serotonin terminal density quantifications (Willoughby and Blessing, 1987; Maddaloni et al., 2017) do not support a regional relationship between rCBV activation and serotonin innervation density. Different serotonin signaling properties, such as a differential contribution of wiring and volume transmission (Descarries and Mechawar, 2000), as well as regional combinations of receptor subtypes characterized by different transductional pathways or cellular distribution may underlie the selective functional engagement observed with endogenous serotonin stimulation. Importantly, our mapping provides functional evidence that serotonergic activation can also modulate the activity of mesolimbic dopaminergic areas such as the nucleus accumbens. This finding underscores a functional interplay between these two key modulatory systems and supports the emerging view of a role of serotonin as a possible modulator of reward processing and mesolimbic dopa-

minergic substrates (Li et al., 2016; Luo et al., 2015). A mechanistic contribution of promiscuous monoaminergic transport could also play a role in the mapped activation, as suggested by recent molecular imaging studies (Hai et al., 2016; Zhou et al., 2005).

Interestingly, recent mapping of chemogenetically stimulated neurons via 2-fluodeoxygucose positron emission tomography (PET) did not highlight corticohippocampal modulation of brain activity, but revealed small foci of reduced metabolism in thalamic areas (Urban et al., 2016). Several experimental factors could account for these discrepant results, including the use of deep anesthesia versus light sedation, and the possible contribution of unspecific effects of CNO, given that Urban et al. did not employ a CNO-treated group as a baseline reference for brain mapping. This aspect is of especial importance in the light of a recent report pointing at a possible role of converted clozapine as primary effector of DREADD-induced manipulations (Gomez et al., 2017). Our pharmacokinetic data are consistent with this view, showing that CNO can be converted to clozapine in vivo. However, several lines of evidence argue against a significant off-target contribution of converted clozapine to our mapping. First, our chemo-fMRI mapping was performed at CNO

Figure 4. Brain-wide fMRI Response to Systemic Citalopram Administration
(A) Anatomical distribution of the brain regions deactivated by citalopram (10 mg/kg) (n = 7) versus vehicle (Z > 1.8, cluster correction p = 0.05) (n = 10).
(B) Illustrative fMRI time course in the prefrontal cortex (mean ± SEM); citalopram was administered at time 0.
(C) rCBV quantification in representative volumes of interest (mean ± SEM, *p < 0.05, **p < 0.01, corrected at q = 0.05).
Cb, cerebellum; Cg, cingulate cortex; DRN, dorsal raphe nucleus; Ent, entorhinal cortex; Hp, hippocampus; Hyp, hypothalamus; mPFC, prefrontal cortex; NAc, nucleus accumbens; SS, somatosensory cortex; Th, thalamus; V1, visual cortex.

doses that negligibly affect fMRI signals. Second, we have quantified and described all chemogenetic responses with respect to a CNO-treated DIO-hMD3q control group of animals. Third, in vivo LFP recordings and microdialysis studies provide evidence of neural responses and extracellular serotonin release in hM3Dq/Pet1-Cre animals, but not in DIO-hM3Dq control animals. Finally, consistent with the notion of "subthreshold clozapine exposure" (Gomez et al., 2017), the measured peak of clozapine concentration is ~25-fold lower the exposure required to obtain behaviorally relevant responses in rodents (Olsen et al., 2008) and below the range of values previously associated with detectable brain exposure in pharmacokinetic studies (Baldessarini et al., 1993). Taken together, these findings strongly argue against a contribution of unspecific clozapine-related effects to the signals mapped with our approach.

Our results provide a reference framework for the interpretation of fMRI imaging studies employing serotonin-targeting agents. In this respect, the divergent functional effects observed with chemogenetic stimulation and serotonin reuptake inhibition are especially relevant, as they suggest that endogenous versus systemic serotonin level boosting can lead to opposing hemodynamic responses, a factor that needs to be taken into account when hemodynamic readouts are used as surrogates for serotonin induced neural manipulations. Serotonin is a key mediator of central and peripheral vasoactivity, with predominant evidence of a vasoconstrictive action via serotonin$_{1A}$, serotonin$_{1B}$ and

serotonin$_{2A}$ receptors located in brain and peripheral vascular cells (reviewed by Cohen et al., 1996). Because serotonin reuptake inhibition rapidly increases circulating levels of this neurotransmitter (Blardi et al., 2005; Zolkowska et al., 2008) and systemic serotonin administration produces endothelial vasoconstriction (Toda and Fujita, 1973; Cohen et al., 1996), citalopram-induced rCBV decreases could reflect a contribution of direct vasoactive effect of circulating serotonin on cerebral vasculature. Nonvascular mechanisms could also be involved in this effect, such as a possible engagement of different receptor populations as a function of serotonin release site, a hypothesis consistent with the wide variety in the anatomical and cellular distribution patterns exhibited by the serotonin receptor subtypes identified thus far (Lesch and Waider, 2012).

While reduced cerebral blood flow in humans and rats has been reported upon citalopram administration (McBean et al., 1999; Geday et al., 2005), prior blood-oxygen-level-dependent (BOLD) fMRI mapping of citalopram in rats revealed increased cortical responses (Sekar et al., 2011). A number of methodological discrepancies could account for this result, the two most notable being the use of deeper anesthesia levels by Sekar et al., as well as the use of BOLD fMRI, as opposed to rCBV (like in the present work). In this respect, it should be emphasized that CBV is a direct and reliable indicator of microvascular activity that appears to be more directly related to underlying neuronal activity than BOLD fMRI (Schridde et al., 2008). Further opto- or chemogenetic

fMRI mapping of serotonin function employing BOLD fMRI could help conciliate these experimental discrepancies.

The results of our microdialysis and LFP recordings, plus the observation of c-Fos induction in many regions exhibiting significant chemo-fMRI activation argue against a significant interference of anesthesia on our functional mapping, and support a neural origin of the mapped signals. Not surprisingly, discrepancies between imaging and c-Fos mapping were noted (e.g., in cortical regions or the cerebellum). Such differences are not surprising given the diverse neurophysiological mechanisms underlying these two experimental readouts and previous evidence showing that c-Fos induction does not always correspond to activation shown by metabolic or hemodynamic-based brain mapping (Stark et al., 2006; Gozzi et al., 2012; Gass et al., 1997). Indeed, hemodynamic responses are generally thought to reflect local synaptic input (Logothetis et al., 2001), whereas the c-Fos protein induction is an indirect marker of cellular activation that is not elicited in all CNS cells and can be affected by the behavioral state of the animal (Cirelli and Tononi, 2000).

From a methodological standpoint, this work paves the way to the combined use of chemogenetics and fMRI to unravel the large-scale substrates modulated by pan-neuronal populations in the living mouse brain. Our approach follows analogous attempts to combine chemogenetics with noninvasive mouse brain imaging (Urban et al., 2016). Our data demonstrate that properly controlled chemogenetic-fMRI studies can elicit large and sustained functional responses that exhibit neuronal specificity and can be employed to noninvasively map the brain-wide effect of regional neural manipulations. This approach crucially complements current opto-fMRI stimulations (Lee et al., 2010) by permitting brain-wide functional mapping without the need for invasive cranial probes, and it is devoid of the confounding contribution of heat-induced vasodilation in anesthetized animals (Rungta et al., 2017). As such, chemo-fMRI appears to be optimally suited to the investigation of drug-like sustained modulatory stimulation/inhibition and for the deconstruction or manipulation of steady-state network activity via fMRI connectivity mapping (Gozzi and Schwarz, 2016). While here employed to study pan-neuronal serotonin modulation, this approach can be straightforwardly expanded to manipulate focal circuits and neuronal ensembles via intersectional genetics or retrograde viral vectors.

In conclusion, we describe the use of chemo-fMRI to map the brain-wide substrates of modulatory transmission in the intact mammalian brain. We show that chemogenetic stimulation of endogenous serotonin neurons results in regionally specific activation of a set of cortical and subcortical targets that serve as primary functional mediators of sustained endogenous serotonin transmission. We also show that endogenous activation of serotonergic neurons and systemic serotonin reuptake inhibition can produce opposing hemodynamic effects. Our findings provide a framework for understanding serotonin-dependent functions and interpreting data obtained from human fMRI studies of serotonin modulating agents.

EXPERIMENTAL PROCEDURES

A complete description of the experimental procedures used can be found in Supplemental Experimental Procedures.

Ethics Statement
All research involving animals were carried out in accordance with the European directive 86/609/EEC governing animal welfare and protection, acknowledged by the Italian Legislative Decree no. 116 (27 January 1992). Animal research protocols were also reviewed and approved by a local animal care committee.

Mouse Line Generation
The hM3Dq sequence fused with mCherry was isolated by a pAAV-hSyn-DIO-hM3Dq construct (a kind gift from Dr. Bryan Roth) and inversely cloned into the ROSA26 locus (Krashes et al., 2011). PvuI-linearized pROSA26-1^{Sor}-LA-CAG-DIO-hM3Dq-NEO-RA-DTa was electroporated in E14Tg2a.4 embryonic stem cells (ESCs). To enable the expression of hM3Dq in serotonin-producing neurons, mice were then crossed with Pet1$_{210}$-Cre mice (Pelosi et al., 2014).

Immunohistochemical Analyses and Cell Counting
Free-floating sections were incubated at 4°C overnight with rabbit anti-RFP (ab62341, Abcam, 1:500) and goat anti-Tph2 (ab121020, Abcam, 1:800). Sections were then incubated with donkey anti-rabbit (rhodamine red, Invitrogen, 1:500) and anti-goat (Alexa Fluor 488, Invitrogen, 1:500). c-Fos mapping was carried out as using a goat anti-c-Fos (SC-52-G, Santa Cruz Biotechnology, 1:1,000) in a 5% horse inactivated serum solution. Sections were then incubated overnight at 4°C with donkey anti-goat (Alexa Fluor 488, Invitrogen, 1:500).

Brain Slice Electrophysiology
Brains of hM3Dq/Pet1-Cre were sectioned to obtain 300-μm coronal slices encompassing the dorsal raphe nucleus. Whole-cell patch-clamp experiments were performed using borosilicate electrodes to patch DRN cells. After 5 min of stable baseline, CNO (10 μM) was bath applied for 10 min while recording changes in membrane potential.

fMRI
Animal preparation for fMRI has been previously described (Sforazzini et al., 2014; Liska et al., 2015). All drugs were administered intravenously. fMRI data were acquired on a 7T Pharmascan using intrapulmonary halothane anesthesia (0.8%) and analyzed as previously described (Galbusera et al., 2017). Images were sensitized to reflect alterations in rCBV using Molday Ion (Biopal).

In Vivo Electrophysiology
LFP recordings were performed on a separate cohort of halothane anaesthetized DIO/hM3Dq or hM3Dq/Pet1-Cre mice using the same animal preparation and anesthesia employed for fMRI. Surgery, recordings, and data analyses were carried out as previously described (Galbusera et al., 2017).

In Vivo Brain Microdialysis
Microdialysis experiments were performed as recently described (Managò et al., 2016). Mice were implanted with concentric dialysis probes in the dorsal hippocampus. Microdialysis experiments were performed upon intraperitoneal administration of CNO (2 mg/kg). Dialysate samples (20 μL) were analyzed using a high-performance liquid chromatography (HPLC) apparatus and a colorimetric electrochemical detector to quantify serotonin.

Pharmacokinetic Measurements
Blood samples (100 μL) were collected from C57BL/6J mice at different time points (15, 30, and 60 min). Plasma levels of clozapine-N-oxide, clozapine, and dimethyl-clozapine were monitored on the Acquity UPLC/MS TQD system consisting of a triple quadrupole detector (TQD) mass spectrometer equipped with an electrospray ionization interface (Olsen et al., 2008). Compounds were quantified by monitoring their multiple reaction monitoring (MRM) peak areas.

Statistical Methods
Voxelwise group statistical analysis of fMRI data were performed with FEAT version 5.63 using a boxcar input function that captured the main alterations in the rCBV signal observed upon compound injection. Maps were thresholded at a significance level of $Z > 1.8$, followed by a cluster correction with a

significance level of p = 0.05. Microdialysis data were analyzed with a 2-way ANOVA for repeated measurements using a significance level α = 0.05. Inter-group differences in LFP recordings were assessed using linear regression followed by a slope analysis using Prism GraphPad version 7.02. c-Fos quantifications were performed using a Student's t test following a false discovery rate correction at q = 0.05.

SUPPLEMENTAL INFORMATION

Supplemental Information includes Supplemental Experimental Procedures and seven figures and can be found with this article online at https://doi.org/10.1016/j.celrep.2017.09.087.

AUTHOR CONTRIBUTIONS

ACKNOWLEDGMENTS

REFERENCES

Anderson, I.M., McKie, S., Elliott, R., Williams, S.R., and Deakin, J.F.W. (2008). Assessing human 5-HT function in vivo with pharmacoMRI. Neuropharmacology 55, 1029–1037.

Armbruster, B.N., Li, X., Pausch, M.H., Herlitze, S., and Roth, B.L. (2007). Evolving the lock to fit the key to create a family of G protein-coupled receptors potently activated by an inert ligand. Proc. Natl. Acad. Sci. USA 104, 5163–5168.

Baldessarini, R.J., Centorrino, F., Flood, J.G., Volpicelli, S.A., Huston-Lyons, D., and Cohen, B.M. (1993). Tissue concentrations of clozapine and its metabolites in the rat. Neuropsychopharmacology 9, 117–124.

Blardi, P., de Lalla, A., Urso, R., Auteri, A., Dell'Erba, A., Bossini, L., and Castrogiovanni, P. (2005). Activity of citalopram on adenosine and serotonin circulating levels in depressed patients. J. Clin. Psychopharmacol. 25, 262–266.

Cirelli, C., and Tononi, G. (2000). On the functional significance of c-fos induction during the sleep-waking cycle. Sleep 23, 453–469.

Cohen, Z., Bonvento, G., Lacombe, P., and Hamel, E. (1996). Serotonin in the regulation of brain microcirculation. Prog. Neurobiol. 50, 335–362.

Descarries, L., and Mechawar, N. (2000). Ultrastructural evidence for diffuse transmission by monoamine and acetylcholine neurons of the central nervous system. Prog. Brain Res. 125, 27–47.

Galbusera, A., De Felice, A., Girardi, S., Bassetto, G., Maschietto, M., Nishimori, K., Chini, B., Papaleo, F., Vassanelli, S., and Gozzi, A. (2017). Intranasal oxytocin and vasopressin modulate divergent brainwide functional substrates. Neuropsychopharmacology 42, 1420–1434.

Gass, P., Bruehl, C., Herdegen, T., Kiessling, M., Lutzenburg, M., and Witte, O.W. (1997). Induction of FOS and JUN proteins during focal epilepsy: congruences with and differences to [14C]deoxyglucose metabolism. Brain Res. Mol. Brain Res. 46, 177–184.

Geday, J., Hermansen, F., Rosenberg, R., and Smith, D.F. (2005). Serotonin modulation of cerebral blood flow measured with positron emission tomography (PET) in humans. Synapse 55, 224–229.

Gomez, J.L., Bonaventura, J., Lesniak, W., Mathews, W.B., Sysa-Shah, P., Rodriguez, L.A., Ellis, R.J., Richie, C.T., Harvey, B.K., Dannals, R.F., et al. (2017). Chemogenetics revealed: DREADD occupancy and activation via converted clozapine. Science 357, 503–507.

Gozzi, A., and Schwarz, A.J. (2016). Large-scale functional connectivity networks in the rodent brain. Neuroimage 127, 496–509.

Gozzi, A., Colavito, V., Seke Etet, P.F., Montanari, D., Fiorini, S., Tambalo, S., Bifone, A., Zucconi, G.G., and Bentivoglio, M. (2012). Modulation of frontocortical activity by modafinil: a functional imaging and fos study in the rat. Neuropsychopharmacology 37, 822–837.

Hai, A., Cai, L.X., Lee, T., Lelyveld, V.S., and Jasanoff, A. (2016). Molecular fMRI of serotonin transport. Neuron 92, 754–765.

Klomp, A., Tremoleda, J.L., Schrantee, A., Gsell, W., and Reneman, L. (2012). The use of pharmacological-challenge fMRI in pre-clinical research: application to the 5-HT system. J. Vis. Exp. 25, 3956.

Krashes, M.J., Koda, S., Ye, C., Rogan, S.C., Adams, A.C., Cusher, D.S., Maratos-Flier, E., Roth, B.L., and Lowell, B.B. (2011). Rapid, reversible activation of AgRP neurons drives feeding behavior in mice. J. Clin. Invest. 121, 1424–1428.

Lee, S.H., and Dan, Y. (2012). Neuromodulation of brain states. Neuron 76, 209–222.

Lee, J.H., Durand, R., Gradinaru, V., Zhang, F., Goshen, I., Kim, D.S., Fenno, L.E., Ramakrishnan, C., and Deisseroth, K. (2010). Global and local fMRI signals driven by neurons defined optogenetically by type and wiring. Nature 465, 788–792.

Lesch, K.-P., and Waider, J. (2012). Serotonin in the modulation of neural plasticity and networks: implications for neurodevelopmental disorders. Neuron 76, 175–191.

Li, Y., Zhong, W., Wang, D., Feng, Q., Liu, Z., Zhou, J., Jia, C., Hu, F., Zeng, J., Guo, Q., et al. (2016). Serotonin neurons in the dorsal raphe nucleus encode reward signals. Nat. Commun. 7, 10503.

Liska, A., Galbusera, A., Schwarz, A.J., and Gozzi, A. (2015). Functional connectivity hubs of the mouse brain. Neuroimage 115, 281–291.

Liu, Z., Zhou, J., Li, Y., Hu, F., Lu, Y., Ma, M., Feng, Q., Zhang, J.-E., Wang, D., Zeng, J., et al. (2014). Dorsal raphe neurons signal reward through 5-HT and glutamate. Neuron 81, 1360–1374.

Logothetis, N.K., Pauls, J., Augath, M., Trinath, T., and Oeltermann, A. (2001). Neurophysiological investigation of the basis of the fMRI signal. Nature 412, 150–157.

Luo, M., Zhou, J., and Liu, Z. (2015). Reward processing by the dorsal raphe nucleus: 5-HT and beyond. Learn. Mem. 22, 452–460.

Maddaloni, G., Bertero, A., Pratelli, M., Barsotti, N., Boonstra, A., Giorgi, A., Migliarini, S., and Pasqualetti, M. (2017). Development of serotonergic fibers in the post-natal mouse brain. Front. Cell. Neurosci. 11, 202.

Managò, F., Mereu, M., Mastwal, S., Mastrogiacomo, R., Scheggia, D., Emanuele, M., De Luca, M.A., Weinberger, D.R., Wang, K.H., and Papaleo, F. (2016). Genetic disruption of Arc/Arg3.1 in mice causes alterations in dopamine and neurobehavioral phenotypes related to schizophrenia. Cell Rep. 16, 2116–2128.

Martin, C., and Sibson, N.R. (2008). Pharmacological MRI in animal models: a useful tool for 5-HT research? Neuropharmacology 55, 1038–1047.

McBean, D.E., Ritchie, I.M., Olverman, H.J., and Kelly, P.A.T. (1999). Effects of the specific serotonin reuptake inhibitor, citalopram, upon local cerebral blood flow and glucose utilisation in the rat. Brain Res. *847*, 80–84.

Ofek, K., Schoknecht, K., Melamed-Book, N., Heinemann, U., Friedman, A., and Soreq, H. (2012). Fluoxetine induces vasodilatation of cerebral arterioles by co-modulating NO/muscarinic signalling. J. Cell. Mol. Med. *16*, 2736–2744.

Olsen, C.K., Brennum, L.T., and Kreilgaard, M. (2008). Using pharmacokinetic-pharmacodynamic modelling as a tool for prediction of therapeutic effective plasma levels of antipsychotics. Eur. J. Pharmacol. *584*, 318–327.

Park, H.G., and Carmel, J.B. (2016). Selective manipulation of neural circuits. Neurotherapeutics *13*, 311–324.

Pelosi, B., Migliarini, S., Pacini, G., Pratelli, M., and Pasqualetti, M. (2014). Generation of Pet1210-Cre transgenic mouse line reveals non-serotonergic expression domains of Pet1 both in CNS and periphery. PLoS ONE *9*, e104318.

Rungta, R.L., Osmanski, B.-F., Boido, D., Tanter, M., and Charpak, S. (2017). Light controls cerebral blood flow in naive animals. Nat. Commun. *8*, 14191.

Schridde, U., Khubchandani, M., Motelow, J.E., Sanganahalli, B.G., Hyder, F., and Blumenfeld, H. (2008). Negative BOLD with large increases in neuronal activity. Cereb. Cortex *18*, 1814–1827.

Sekar, S., Verhoye, M., Van Audekerke, J., Vanhoutte, G., Lowe, A.S., Blamire, A.M., Steckler, T., Van der Linden, A., and Shoaib, M. (2011). Neuroadaptive responses to citalopram in rats using pharmacological magnetic resonance imaging. Psychopharmacology (Berl.) *213*, 521–531.

Sforazzini, F., Schwarz, A.J., Galbusera, A., Bifone, A., and Gozzi, A. (2014). Distributed BOLD and CBV-weighted resting-state networks in the mouse brain. Neuroimage *87*, 403–415.

Spencer, W.C., and Deneris, E.S. (2017). Regulatory mechanisms controlling maturation of serotonin neuron identity and function. Front. Cell. Neurosci. *11*, 215.

Stark, J.A., Davies, K.E., Williams, S.R., and Luckman, S.M. (2006). Functional magnetic resonance imaging and c-Fos mapping in rats following an anorectic dose of m-chlorophenylpiperazine. Neuroimage *31*, 1228–1237.

Takahashi, A., Quadros, I.M., De Almeida, R.M.M., and Miczek, K.A. (2012). Behavioral and pharmacogenetics of aggressive behavior. In Behavioral Neurogenetics, J.F. Cryan and A. Reif, eds. (Springer Berlin Heidelberg).

Toda, N., and Fujita, Y. (1973). Responsiveness of isolated cerebral and peripheral arteries to serotonin, norepinephrine, and transmural electrical stimulation. Circ. Res. *33*, 98–104.

Underwood, M.D., Bakalian, M.J., Arango, V., and Mann, J.J. (1995). Effect of chemical stimulation of the dorsal raphe nucleus on cerebral blood flow in rat. Neurosci. Lett. *199*, 228–230.

Urban, D.J., Zhu, H., Marcinkiewcz, C.A., Michaelides, M., Oshibuchi, H., Rhea, D., Aryal, D.K., Farrell, M.S., Lowery-Gionta, E., Olsen, R.H., et al. (2016). Elucidation of the behavioral program and neuronal network encoded by dorsal raphe serotonergic neurons. Neuropsychopharmacology *41*, 1404–1415.

Willoughby, J.O., and Blessing, W.W. (1987). Origin of serotonin innervation of the arcuate and ventromedial hypothalamic region. Brain Res. *418*, 170–173.

Zhou, F.-M., Liang, Y., Salas, R., Zhang, L., De Biasi, M., and Dani, J.A. (2005). Corelease of dopamine and serotonin from striatal dopamine terminals. Neuron *46*, 65–74.

Zolkowska, D., Baumann, M.H., and Rothman, R.B. (2008). Chronic fenfluramine administration increases plasma serotonin (5-hydroxytryptamine) to nontoxic levels. J. Pharmacol. Exp. Ther. *324*, 791–797.